

CONF-9709161--

Appendix XIII "Magnetic Breakdown and Landau Level Spectra of a Tunable Double-Quantum-Well Fermi Surface"

**MASTER**  
JA

DISTRIBUTION OF THIS DOCUMENT IS UNLIMITED

### **DISCLAIMER**

This report was prepared as an account of work sponsored by an agency of the United States Government. Neither the United States Government nor any agency thereof, nor any of their employees, makes any warranty, express or implied, or assumes any legal liability or responsibility for the accuracy, completeness, or usefulness of any information, apparatus, product, or process disclosed, or represents that its use would not infringe privately owned rights. Reference herein to any specific commercial product, process, or service by trade name, trademark, manufacturer, or otherwise does not necessarily constitute or imply its endorsement, recommendation, or favoring by the United States Government or any agency thereof. The views and opinions of authors expressed herein do not necessarily state or reflect those of the United States Government or any agency thereof.

## **DISCLAIMER**

**Portions of this document may be illegible in electronic image products. Images are produced from the best available original document.**

## Magnetic breakdown and Landau level spectra of a tunable double-quantum-well Fermi surface

J. A. Simmons,<sup>a</sup> N. E. Harff,<sup>a,\*</sup> S. K. Lyo,<sup>a</sup>  
G. S. Boebinger,<sup>b</sup> J. F. Klem,<sup>a</sup> L. N. Pfeiffer,<sup>b</sup> and K. W. West<sup>b</sup>

*a) Sandia National Laboratories, Albuquerque, NM 87185 USA*

*b) Bell Laboratories, Lucent Technologies, Murray Hill, NJ 07974 USA*

By measuring longitudinal resistance, we map the Landau level spectra of double quantum wells as a function of both parallel ( $B_{\parallel}$ ) and perpendicular ( $B_{\perp}$ ) magnetic fields. In this continuously tunable highly non-parabolic system, the cyclotron masses of the two Fermi surface orbits change in opposite directions with  $B_{\parallel}$ . This causes the two corresponding ladders of Landau levels formed at finite  $B_{\perp}$  to exhibit multiple crossings. We also observe a third set of Landau levels, independent of  $B_{\parallel}$ , which arise from magnetic breakdown of the Fermi surface. Both semiclassical and full quantum mechanical calculations show good agreement with the data.

Interest in double quantum wells (DQWs) has been growing for the past several years. Recently it was shown that at sufficiently high in-plane magnetic fields  $B_{\parallel}$ , closely-coupled DQWs exhibit an anticrossing in the dispersion curve, leading to additional singularities in the density of states. [1,2] In these experiments, a  $B_{\parallel}$  shifts the two QW Fermi circles relative to one another in  $k$  space, thereby providing a controlled distortion of the two non-circular orbits of the coupled QW Fermi surface (FS). These orbits have been shown to have greatly distorted cyclotron masses which depend strongly on  $B_{\parallel}$ . [3,4] Thus when a perpendicular magnetic field  $B_{\perp}$  is added, [5] the resulting Landau level (LL) spectrum is expected to be unusually complex. The situation is further complicated by magnetic breakdown (MB), in which an electron tunnels in  $k$  space from one FS orbit to the other. [6]

In this work, we experimentally map the LL spectrum of two closely-coupled GaAs/AlGaAs DQW structures by measuring the longitudinal resistance  $R_{xx}$  as a function of both  $B_{\parallel}$  and  $B_{\perp}$ . [7] We observe three separate sets of LLs. The first two sets arise from the two non-circular FS orbits, whose masses and Fermi energies depend strongly on  $B_{\parallel}$ . The third set of LLs, insensitive to  $B_{\parallel}$ , arises from MB of the FS. Both semiclassical and full quantum calculations show good agreement with the data.

The two samples investigated were modulation doped GaAs/Al<sub>0.3</sub>Ga<sub>0.7</sub>As

DQWs, each consisting of two QWs of equal width  $w$  separated by a barrier of thickness  $t$ . Table I lists the  $B_{\parallel}=0$  values for the electron densities in the two lowest subbands ( $n_1$  and  $n_2$ ), the total mobility, and the symmetric-antisymmetric energy gap  $\Delta_{SAS}$ . Standard four-terminal lock-in measurements were performed at 0.3 K. To achieve variation of both  $B_{\perp}$  and  $B_{\parallel}$ , roughly nine hundred sweeps of total magnetic field  $B_T$  are done at different angles  $\theta$  set by an *in situ* rotating stage.  $B_{\parallel}$  and  $B_{\perp}$  were determined using two identically calibrated Hall probes: one measures  $B_T$ , while the other measures  $B_{\perp}$  only.

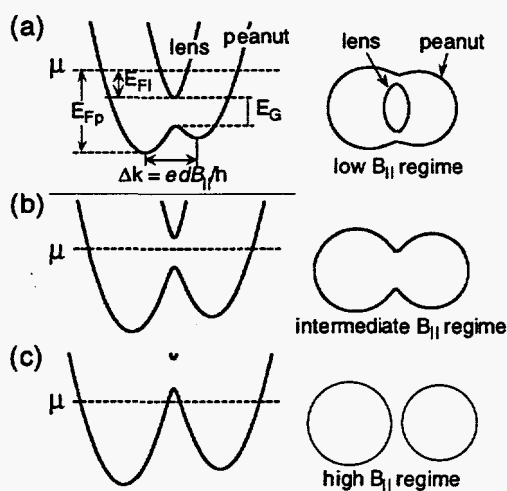


Fig. 1. Sketch of the dispersion (left) and Fermi surface for  $\mu=6.8$  meV (right) for sample A at  $B_{\parallel}=(a)$  5.0 T, (b) 7.0 T, and (c) 9.0 T.

Table 1. Sample parameters.

Sample	w/t (Å)	n (10 <sup>11</sup> cm <sup>-2</sup> )		$\mu_{\text{TOTAL}}$ (cm <sup>2</sup> /Vs)	$\Delta_{\text{SAS}}$ (meV)
		n <sub>1</sub>	n <sub>2</sub>		
A	150/15	1.0	1.9	3.1×10 <sup>5</sup>	2.3
B	139/28	1.9	2.4	7.4×10 <sup>5</sup>	1.5

The main effect of  $B_{\parallel}$  is a linear transverse shift in  $k$ -space  $\Delta k = edB_{\parallel}/h$  of one QW's dispersion curve with respect to that of the other, where  $d$  is the distance between the two electron layers. When the coupling is strong, the two QW dispersion curves anticross and a partial energy gap  $E_G$  appears, where  $E_G \approx \Delta_{\text{SAS}}$ , the symmetric-antisymmetric energy gap. [1,2] Fig. 1 shows a sketch of the dispersion curve and FS for sample A at each of three distinct  $B_{\parallel}$  regimes. At low  $B_{\parallel}$  the energy gap is below  $\mu$ , and the FS has an inner lens-shaped orbit and an outer peanut-shaped orbit.  $\Delta k$  increases with  $B_{\parallel}$ , moving the gap upwards in energy and also decreasing the Fermi energy of the lens orbit  $E_{\text{Fl}}$ . By contrast, the peanut Fermi energy  $E_{\text{Fp}}$  only depends slowly on  $B_{\parallel}$ . For intermediate  $B_{\parallel}$ ,  $\mu$  resides in the gap, and the FS contains only the peanut orbit. Finally, at high  $B_{\parallel}$  the bottom of the energy gap moves above  $\mu$  and the FS now consists of two uncoupled circular orbits.

Fig. 2 shows gray-scale plots of  $R_{xx}(B_{\parallel}, B_{\perp})$  measured for both samples. (The overlaid thin black lines are a semiclassical calculation to be discussed below.) For sample A, the data spans all three regimes: high  $B_{\parallel}$  ( $>7.5$  T), intermediate  $B_{\parallel}$  ( $6.0$  T  $< B_{\parallel} < 7.5$  T), and low  $B_{\parallel}$  ( $< 6.0$  T). For sample B, only the low  $B_{\parallel}$  ( $< 9.0$  T) and part of the intermediate  $B_{\parallel}$  ( $> 9.0$  T) regimes are present. We first discuss the high  $B_{\parallel}$  regime. Here oscillations versus  $B_{\perp}$  are nearly independent of  $B_{\parallel}$ , resulting in a set of vertical high resistance ridges. This is as expected since the energy gap is above  $\mu$ : the FS consists of two well-separated circle orbits [Fig. 1(c)] whose sizes do not change with  $B_{\parallel}$ .

The low  $B_{\parallel}$  regime exhibits a more complex  $R_{xx}$  which depends strongly on  $B_{\parallel}$ . High resistance ridges, running from upper left to lower right, are due to LLs from the lens orbit coinciding with  $\mu$ . This clear

depopulation of lens LLs with  $B_{\parallel}$  is due to two effects. First, as  $B_{\parallel}$  is increased,  $E_{\text{Fl}}$  decreases. Second, there is a concurrent increase in the lens LL energy spacing  $\hbar\omega_{c1} = eB_{\perp}/m^*_1$ , due to the decrease in  $m^*_1$  arising from the distorted dispersion. [3,4] A second weaker set of high resistance ridges, running from lower left to upper right, is also apparent, especially in the expanded view of

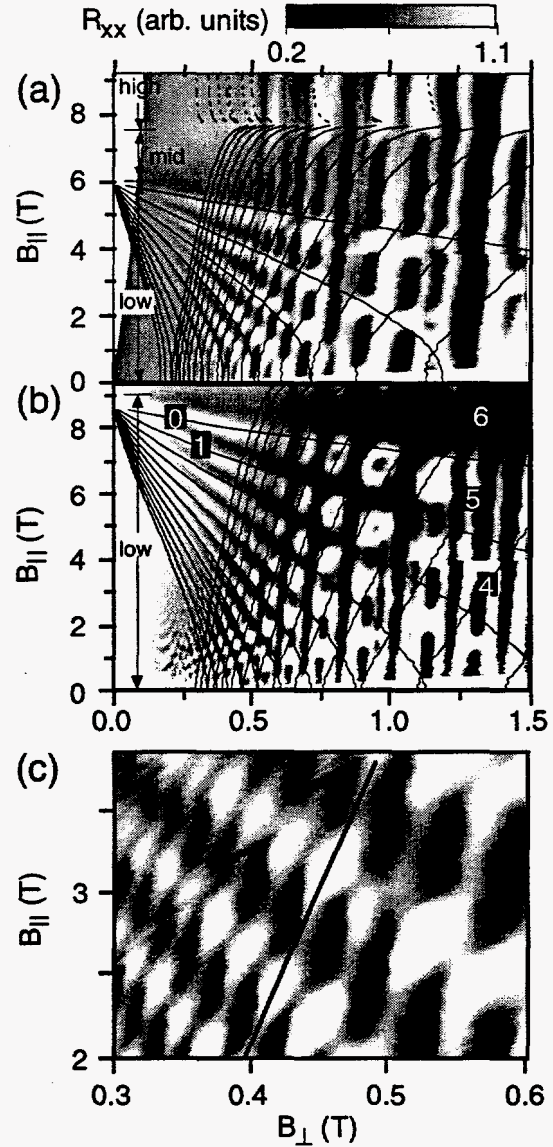


Fig. 2. Gray-scale: measured  $R_{xx}(B_{\parallel}, B_{\perp})$  for (a) sample A, and (b) sample B. Overlaid thin black lines are the semiclassical calculation. In (b) the  $N=0$  and  $N=1$  lens and  $N=4, 5,$  and  $6$  peanut LLs are labeled. The  $B_{\parallel}$  regimes are indicated. (c) Expanded view of the data for sample A, with the range of the gray scale reduced to enhance the contrast. The black line indicates a single peanut LL.

$R_{xx}(B_{||}, B_{\perp})$  for sample A shown in Fig. 3(c). These ridges are due to the peanut orbit, which is so large that relatively few electrons can complete it without scattering. In contrast to the lens, the filling factor of the peanut LLs increases with  $B_{||}$  while  $E_{FP}$  only changes slowly with  $B_{||}$ , the peanut cyclotron mass  $m^*_p$  increases strongly, [3,4] causing a decrease in the peanut LL energy separation  $\hbar\omega_{cp} = eB_{\perp}/m^*_p$ . Finally, a third set of  $R_{xx}$  ridges runs nearly vertically. This set is due

to MB, in which electrons tunnel between the lens and peanut orbits so as to form circular orbits corresponding to the individual QWs. While these vertical ridges are relatively weak at low  $B_{\perp}$ , their strength increases rapidly so that they dominate  $R_{xx}$  at high  $B_{\perp}$ , as expected. [6,7]

At intermediate  $B_{||}$ , only vertical ridges appear. Here  $\mu$  lies in the energy gap and only the peanut orbit is present. We also attribute these vertical ridges to MB, except in this case electrons form circular orbits by tunneling across the neck of the peanut orbit. The peanut orbit itself produces only slight wiggles in the vertical  $R_{xx}$  ridges, occurring whenever a peanut LL crosses a LL due to MB.

Our overall explanation of  $R_{xx}(B_{||}, B_{\perp})$  is further supported by Figs. 3(a) and 3(b), which show Fourier power spectra in  $1/B_{\perp}$  of the data of Figs. 2(a) and 2(b), over the range  $0.1 < B_{\perp} < 1.2$  T. For both samples, a low frequency lens orbit peak and a high frequency peanut orbit peak are clearly seen. As  $B_{||}$  is increased, the lens (peanut) peak moves to smaller (larger) frequencies, indicating a decreasing (increasing) area in  $k$ -space. Two intermediate frequency peaks are also seen. These peaks are due to MB between the lens and peanut orbits, and remain relatively unchanged with  $B_{||}$ . [7] At low  $B_{||}$ , sample B exhibits significant MB. Sample A, on the other hand, shows a strong peanut peak but does not as clearly resolve the two intermediate QW frequencies until the high  $B_{||}$  regime, because its larger  $\Delta S_{AS}$  inhibits MB. [6,7] The presence of MB is further illustrated by Fig. 3(c), which also shows a Fourier power spectrum for sample B, but only over the range  $0.1 < B_{\perp} < 0.5$  T. The relative strength of the intermediate frequency QW peaks is greatly reduced, consistent with MB occurring only at higher  $B_{\perp}$ . [6,7]

To test our model, we semiclassically calculate the  $B_{||}, B_{\perp}$  values at which the lens and peanut LLs cross  $\mu$ . The DQW potential is obtained from the flat-band potential of the growth structures by adjusting the depth of each QW to obtain the measured (uncoupled) densities. An equal but opposite amount of linear band bending is then artificially added to each QW so as to yield the measured  $\Delta S_{AS}$

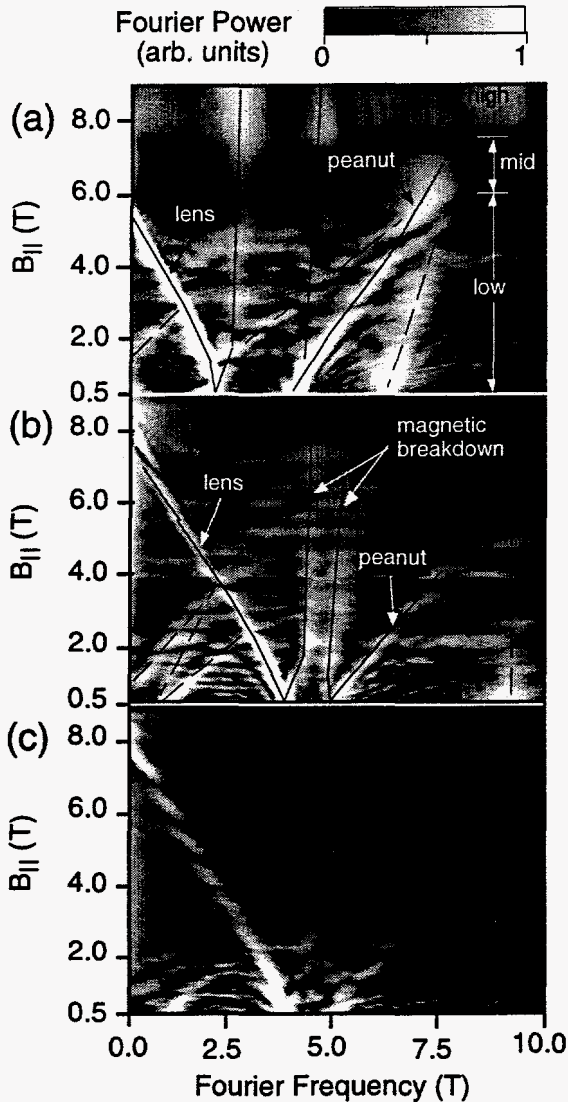


Fig. 3. Fourier power in  $1/B_{\perp}$  of the data of Fig. 2, for (a) sample A, and (b) sample B, for  $0.1 < B_{\perp} < 1.2$  T. Overlaid black lines are guides to the eye, indicating the primary orbit peaks (solid) and secondary peaks corresponding to sums and differences of the primaries (dashed). In (a) the  $B_{||}$  regimes are indicated. (c) Same as (b), but only for  $0.1 < B_{\perp} < 0.5$  T.

value. (A Hartree calculation gives only minor differences in results.) The DQW potential thus obtained is then used to find the uncoupled QW wavefunctions and eigenvalues, which are then used in a tight-binding calculation of the DQW dispersion  $E(k_x, k_y, B_{\parallel})$  following Lyo. [1,4] From  $E(k_x, k_y, B_{\parallel})$  we obtain  $E_{F1}(B_{\parallel})$  (making the approximation that  $E_{Fp}(B_{\parallel})$  and  $\mu$  are constant) and also the cyclotron masses  $m^*_{1,p}(B_{\parallel}) = (\hbar^2/2\pi)\partial A_{1,p}/\partial E$ , where  $A_{1,p}$  is the area in  $k$  space of the (lens or peanut) orbit evaluated at  $\mu$ . The LL energies are then given by  $E_{F1,p} = (N_{1,p} + 1/2)\hbar e B_{\perp} / m^*_{1,p}(B_{\parallel})$ , where the LL index  $N_{1,p} = 0, 1, 2, \dots$ . This approach makes the approximation that each energy branch is well-described by a constant  $m^*_{1,p}$  for each  $B_{\parallel}$ . The  $B_{\parallel}, B_{\perp}$  values at which the LLs cross  $\mu$  are then obtained by fixing  $N_{1,p}$  and  $B_{\parallel}$ , and finding the  $B_{\perp}$  which makes this relation an equality.

The results of this calculation are shown as thin black lines in Figs. 2(a) and 2(b). All the essential features of the experimental data, in particular the approximate positions of the lens and peanut LLs, are reproduced. The sharp  $R_{xx}$  peaks in the data correspond closely with the calculated intersection points of the lens and peanut LLs. [7] The calculation's unusual behavior near  $B_{\parallel} = 7.5$  T for sample A is due to the saddle point in the peanut dispersion branch, where  $m^*_p$  diverges logarithmically. [1-4]

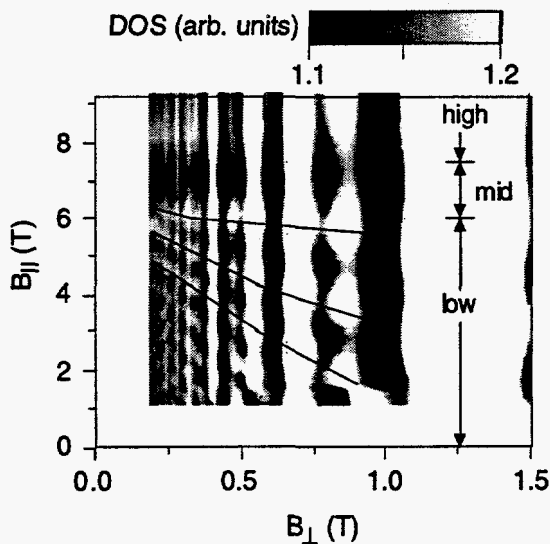


Fig. 4. Results of a full quantum calculation of the density of states as a function of  $B_{\parallel}$  and  $B_{\perp}$  for a sample similar to A. Black lines indicate lens LLs.

We also performed a full quantum-mechanical calculation of the density of states at  $\mu$ , diagonalizing the tight-binding Hamiltonian of Hu and MacDonald. [6] This Hamiltonian consists of diagonal elements which represent Landau ladders  $(N+1/2)\hbar\omega_{\perp}$  of the two QWs displaced in energy by  $E_{1,2}$ , and inter-ladder (i.e., inter-QW) off-diagonal elements which couple any two rungs of the ladders. Here, the cyclotron frequency is given by  $\omega_{\perp} = eB_{\perp}/m^*$ . A Gaussian lineshape is assumed for each level of the eigenvalues, with a root mean-square deviation  $\sigma = \Gamma/2$ . Here, the full level width  $\Gamma$  due to impurity damping is given by  $\Gamma = 0.5\hbar\omega_{\perp}/\sqrt{B_{\perp}}$ , where  $B_{\perp}$  is in units of T. [8] The results of this calculation are shown in Fig. 4 for a structure similar to sample A, using  $n_1 = 0.8 \times 10^{11} \text{ cm}^{-2}$ ,  $n_2 = 1.6 \times 10^{11} \text{ cm}^{-2}$ , and  $\Delta_{SAS} = 2.0 \text{ meV}$ . The salient features of the data are reproduced, with large peaks in the DOS occurring whenever LLs from each FS branch overlap at  $\mu$ . The results for sample B, as well as calculations of  $R_{xx}$  using linear response theory, yield similar satisfactory agreement. Details will be published elsewhere. [9]

### Acknowledgements

Sandia is a multiprogram laboratory operated by the Sandia Corp., a Lockheed-Martin company, for the U. S. Dept of Energy under Contract DE-AC04-94AL85000.

### References

- \* Present address: Max Planck Institute, Stuttgart, Germany.
- [1] S. K. Lyo, Phys. Rev. B 50 (1994) 4965.
- [2] J. A. Simmons, S. K. Lyo, N. E. Harff, and J. F. Klem, Phys. Rev. Lett. 73 (1994) 2256.
- [3] J. A. Simmons, N. E. Harff, and J. F. Klem, Phys. Rev. B 51 (1995) 11156.
- [4] S. K. Lyo, Phys. Rev. B 51 (1995) 11160.
- [5] G. S. Boebinger *et al.*, Phys. Rev. B 43 (1991) 12673.
- [6] J. Hu and A. H. MacDonald, Phys. Rev. B 46 (1992) 12554.
- [7] N. E. Harff *et al.*, Phys. Rev. B 55 (1997) R13405.
- [8] T. Uenoyama and L. J. Sham, Phys. Rev. B 39 (1989) 11044.
- [9] S. K. Lyo *et al.*, unpublished.

## APPENDIX I: List of Refereed Publications and Presentations

### Refereed Publications:

1. M. V. Weckwerth, J. A. Simmons, N. E. Harff, M. E. Sherwin, M. A. Blount, W. E. Baca, and H. C. Chui, 1996. "Epoxy bond and stop-etch (EBASE) technique enabling backside processing of (Al)GaAs heterostructures," *Superlattices and Microstructures* **20**, 561.
2. J. A. Simmons, M. A. Blount, J. S. Moon, W. E. Baca, J. L. Reno, and M. J. Hafich, 1997. "Unipolar Complementary Bistable Memories Using Gate-Controlled Negative Differential Resistance in a 2D-2D Quantum Tunneling Transistor," *IEEE Technical Digest of the 1997 International Electron Devices Meeting*, Washington DC, Dec. 7-10, p. 755.
3. J. S. Moon, J. A. Simmons, M. A. Blount, W. E. Baca, J. L. Reno, and M. J. Hafich, 1997. "Compact Logic/Memory Elements Using a Gated 2D-2D Quantum Tunneling Transistor," *Proceedings of the 1997 International Semiconductor Device Research Symposium*, Charlottesville, Virginia, Dec. 10-13, p. 27.
4. J. A. Simmons, M. A. Blount, J. S. Moon, S. K. Lyo, W. E. Baca, J. R. Wendt, J. L. Reno, and M. J. Hafich, 1998. "A Planar Transistor Based on 2D-2D Tunneling in a Double Quantum Well Heterostructure," submitted to *Nature*.
5. J. S. Moon, J. A. Simmons, M. A. Blount, W. E. Baca, J. L. Reno, and M. J. Hafich, 1998. "Gate Controlled Double Electron Layer Tunneling Transistor (DELTT) and Single Transistor Digital Logic Applications," to appear in *Electronics Letters*.
6. M. A. Blount, J. A. Simmons, J. S. Moon, W. E. Baca, J. L. Reno, and M. J. Hafich, 1998. "Complementary Bistable Memories Using a Novel Double Electron Layer Tunneling Transistor (DELTT)," to appear in *Semiconductor Science and Technology*.
7. J. R. Wendt, J. A. Simmons, J. S. Moon, W. E. Baca, M. A. Blount, and J. L. Reno, "Dual-Side Electron Beam Lithography for Independent Submicron Gating of Double Quantum Well Devices," to appear in *Semiconductor Science and Technology*.
8. M. A. Blount, J. A. Simmons, and S. K. Lyo, 1998. "In-Plane Magnetoresistance Studies of an Extremely Coupled Double Quantum Well," to appear in *Phys. Rev. B*.



9. N. E. Harff, J. A. Simmons, J. F. Klem, G. S. Boebinger, L. N. Pfeiffer, and K. W. West, 1996. "Observation of Magnetic Breakdown in Double Quantum Wells," *Superlattices and Microstructures* **20**, 595.
10. N. E. Harff, J. A. Simmons, S. K. Lyo, J. F. Klem, G. S. Boebinger, L. N. Pfeiffer, and K. W. West, 1997. "Magnetic Breakdown and Landau-level Spectra of a Tunable Double-Quantum-Well Fermi Surface," *Phys. Rev. B* **55**, R13405.
- X 11. N. E. Harff, J. A. Simmons, S. K. Lyo, J. F. Klem, G. S. Boebinger, L. N. Pfeiffer, and K. W. West, 1997. "Landau Level Formation and Magnetic Breakdown in Coupled Double Quantum Wells," *Physica E* **1**, 185.
12. J. A. Simmons, N. E. Harff, S. K. Lyo, J. F. Klem, G. S. Boebinger, L. N. Pfeiffer, and K. W. West, 1998. "Magnetic Breakdown and Landau Level Spectra of a Tunable Double-Quantum-Well Fermi Surface," to appear in *Physica B*.
13. S. K. Lyo, 1998. "Quantum Oscillations of 2-Dimensional to 2-Dimensional Tunneling in Bilayer Electron Gases in Tilted Magnetic Fields," *Phys. Rev. B* **57**, 9114.
14. S. K. Lyo, N. E. Harff, and J. A. Simmons, 1998. "Magnetoquantum-Resistance Oscillations in Tunnel-Coupled Double Quantum Wells in Tilted Magnetic Fields: Variable Landau Bi-Ladders," to appear in *Phys. Rev. B*.

### **Presentations**

1. N. E. Harff, J. A. Simmons, J. F. Klem, and M. V. Weckwerth, 1996. "Magnetic Breakdown In Coupled Double Quantum Wells," 1996 March Meeting of the American Physical Society, St. Louis, MO, 3/18-22/96.
2. J. A. Simmons, M. E. Sherwin, M. V. Weckwerth, N. E. Harff, T. M. Eiles, W. E. Baca, H. Q. Hou, and B. E. Hammons, 1996. "Advanced Fabrication Technologies For Nanoelectronics," (INVITED), State of the Art Program on Compound Semiconductors XXIV, Electrochemical Society, Los Angeles, CA 5/5-10/96.
3. N. E. Harff, J. A. Simmons, J. F. Klem, G. S. Boebinger, L. N. Pfeiffer, and K. W. West, 1996. "Observation Of Magnetic Breakdown In Double Quantum Wells," NanoMES '96, Santa Fe, NM, 5/19-24/96.
4. M.V. Weckwerth, J. A. Simmons, N. E. Harff, M. E. Sherwin, M. A. Blount, W. E. Baca, and H. C. Chui, 1996. "Epoxy Bond And Stop-Etch (Ebase) Technique Enabling Backside Processing Of (Al)GaAs Heterostructures," NanoMES '96, Santa Fe, NM, 5/19-24/96.

5. N. E. Harff, J. A. Simmons, J. F. Klem, G. S. Boebinger, L. N. Pfeiffer, and K. W. West, 1996. "Magnetic Breakdown In Double Quantum Wells," 23rd International Conference on the Physics of Semiconductors, Berlin, Germany, 7/21-26/96.
6. M. A. Blount, J. A. Simmons, N. E. Harff, S. K. Lyo, and M. J. Hafich, 1997. "Magnetoconductance And Effective Mass Of An Extremely Closely Coupled Double Quantum Well," American Physical Society March Meeting, Kansas City, MO, 3/17-21/97.
7. N. E. Harff, J. A. Simmons, S. K. Lyo, J. F. Klem, G. S. Boebinger, L. N. Pfeiffer, and K. W. West, 1997. "Magnetic Breakdown And Landau Level Spectrum Of Coupled Double Quantum Wells In Tilted Magnetic Fields," American Physical Society March Meeting, Kansas City, MO, 3/17-21/97.
8. J. A. Simmons, W. E. Baca, J. S. Moon, M. A. Blount, and J. R. Wendt, 1997. "Epoxy-Bond-And-Stop-Etch (Ebase) Technique For Close Proximity Submicron Backside Gating Of Algaas/Gaas Heterostructures," American Physical Society March Meeting, Kansas City, MO, 3/17-21/97.
9. N. E. Harff, J. A. Simmons, S. K. Lyo, J. F. Klem, J. R. Wendt, M. A. Blount, W. E. Baca, and T. R. Castillo, 1997. "Electron Transport In Coupled Double Quantum Wells And Wires," Oregon State University (Electrical & Computer Engineering Dept.), Corvallis, Oregon.
10. M. A. Blount, J. A. Simmons, S. K. Lyo, N. E. Harff, and M. V. Weckwerth, 1997. "Magnetoresistance And Cyclotron Mass In Strongly-Coupled Double Quantum Wells Under In-Plane Magnetic Fields," 24th International Symposium on Compound Semiconductors, San Diego, CA, 9/7-11/97.
11. J. A. Simmons, N. E. Harff, S. K. Lyo, J. F. Klem, G. S. Boebinger, L. N. Pfeiffer, and K. W. West, 1997. "Magnetic Breakdown And Landau Level Spectra Of A Tunable Double Quantum Well Fermi Surface," 12th International Conference on the Electronic Properties of Two-Dimensional Systems, Tokyo, Japan, 9/22-26/97.
12. M. A. Blount, J. A. Simmons, J. S. Moon, W. E. Baca, J. R. Wendt, J. L. Reno, and M. J. Hafich, 1998. "Bistable Memory Cells Utilizing The Double Electron Layer Tunneling Transistor (DELTT)," 1998 March American Physical Society Meeting, Los Angeles, CA, 3/16-20/98.
13. J. S. Moon, J. A. Simmons, M. A. Blount, W. E. Baca, J. L. Reno, and M. J. Hafich, 1998. "Single Transistor Digital Logic Circuits Based On Gate-Controlled 2d-2d Resonant Tunneling," 1998 March American Physical Society Meeting, Los Angeles, CA, 3/16-20/98.

14. J. A. Simmons, M. A. Blount, J. S. Moon, W. E. Baca, J. R. Wendt, J. L. Reno, and M. J. Hafich, 1998. "Double Electron Layer Tunneling Transistor (DELTT) Based On Gate Control Of 2d-2d Tunneling," 1998 March American Physical Society Meeting, Los Angeles, CA, 3/16-20/98.